GIS Odyssey Journal

2026 • Volume 6 • Number 2

https://doi.org/10.57599/gisoj.2026.6.2.243

Ľudovít Kovanič[1], Peter Blišťan[2], Kristína Kamenčíková[3], Branislav Topitzer[4], Patrik Peťovský[5], Ondrej Tokarčík[6], František Radinger[7], Jakub Marcin[8]

ANALYSIS OF TLS DATA FOR DETERMINING THE GEOMETRIC PARAMETERS OF OBJECTS IN AN INDUSTRIAL ENVIRONMENT

Abstract: The article addresses the use of terrestrial laser scanning for the documentation and geometric analysis of two homogenizing silos located within a cement plant in eastern Slovakia. It presents the design and implementation of field data acquisition, scan registration workflow, georeferencing using control points, point cloud processing, creation of a polygonal 3D model, and subsequent analysis of height, diameter, verticality, and shell deviations from an ideal cylindrical model. A Leica RTC360 scanner was used for data acquisition, while processing was carried out using several softwrares. Geometric analysis of the silo structure revealed high spatial consistency with an average diameter of 14.833 m along its height. Over an 85 m vertical interval, a maximum axis displacement of 0.262 m was detected, corresponding to a vertical tilt angle of 0.177°. Model comparison with an ideal cylinder yielded an RMSE of 37 mm, with 84% of shell points within a deviation range of –30 mm to +40 mm and a calculated ovality of 0.94%. The results demonstrated the suitability of the proposed approach and presentation format, which may be applied to similar research and technical tasks as well as practice.

Keywords: TLS, point cloud, , silo, verticality, analysis of geometric parameters

Received: 3 July 2026; accepted: 4 August 2026; revised: 15 September 2026

[1] Technical University of Košice, Faculty of Mining, Ecology, Process Control and Geotechnology, Košice, Slovak Republic, ORCID ID: 0000-0003-4763-1013, email: ludovit.kovanic@tuke.sk
[2] Technical University of Košice, Faculty of Mining, Ecology, Process Control and Geotechnology, Košice, Slovak Republic, ORCID ID: 0000-0002-8452-3532, email: peter.blistan@tuke.sk
[3] Technical University of Košice, Faculty of Mining, Ecology, Process Control and Geotechnology, Košice, Slovak Republic, email: kristina.kamencikova@tuke.sk
[4] Technical University of Košice, Faculty of Mining, Ecology, Process Control and Geotechnology, Košice, Slovak Republic, ORCID ID: 0009-0009-2869-9398, email: branislav.topitzer@tuke.sk
[5] Technical University of Košice, Faculty of Mining, Ecology, Process Control and Geotechnology, Košice, Slovak Republic, ORCID ID: 0009-0001-0233-4229, email: patrik.petovsky@tuke.sk
[6] Technical University of Košice, Faculty of Mining, Ecology, Process Control and Geotechnology, Košice, Slovak Republic, ORCID ID: 0009-0000-8739-4505, email: ondrej.tokarcik@tuke.sk
[7] Technical University of Košice, Faculty of Mining, Ecology, Process Control and Geotechnology, Košice, Slovak Republic, email: frantisek.radinger@tuke.sk
[8] Technical University of Košice, Faculty of Mining, Ecology, Process Control and Geotechnology, Košice, Slovak Republic, email: jakub.marcin@tuke.sk

Introduction

Terrestrial laser scanning (TLS) remains one of the modern methods for acquiring spatial data on objects. Its main advantage lies in its ability to rapidly capture a large number of points on an object's surface and thus create a detailed digital model of its geometry in the form of a point cloud. TLS data are applied in geodesy (Bakuła et al., 2022), industrial mapping (Štroner et al., 2025), construction (Štroner et al., 2025; Erdélyi et al., 2020), documentation of technical objects (Urban et al., 2024; Bariczová et al., 2021), as well as in monitoring their condition over time.

Compared with conventional geodetic methods, TLS provides non-selective data acquisition, in which not only a limited number of characteristic points are captured, but also a large portion of the object's surface (Kregar et al., 2022). This is particularly advantageous for objects with complex irregular shapes (Matoušková et al., 2021; Mackiewicz, 2021; Pavelka et al., 2023) or for structures (Kovanič et al., 2020) in which it is necessary to assess not only basic dimensions, but also local deviations, deformations, or surface regularity (Štroner et al., 2022; Gajski et al., 2023; Gajski et al., 2026).

Industrial silos represent a specific category of objects for which accurate knowledge of geometric parameters is important from the perspective of operation, maintenance, and technical documentation. Their basic shape is close to an ideal cylinder; however, the actual condition may be influenced by construction tolerances, technological interventions, local structural elements, or slight deviation of the vertical axis of the object. For this reason, they are a suitable subject for point-cloud-based analysis, which enables simultaneous assessment of both the global geometry and local shell deviations.

TLS is a contactless method for determining the spatial coordinates of points on an object's surface, where the position of a point is typically derived from measurements of slant distance, horizontal angle, and zenith angle, i.e., on the principle of the spatial polar method, which enables efficient determination of point positions in three-dimensional space (Ma et al., 2018).

The result of the measurement is a point cloud representing the object's surface. The quality of this output depends on instrument accuracy, measurement geometry, point density, surface properties of the object, and environmental conditions during data acquisition. Therefore, in every TLS application, it is important to pay attention not only to the parameters of the instrument used, but also to the design of scan positions, registration, and subsequent data preprocessing (Kovanič et al., 2023; Casula et al., 2026).

For objects with an approximately cylindrical shape, geometric analysis can be based on cross-sections, in which circle fitting is performed. From the centers and radii thus determined, information on diameter, the course of the object axis, verticality, and shell deviations with respect to the ideal model can subsequently be derived (Kovanič et al., 2023). This principle was also used in the presented study.

The objects of the research are homogenization silos located in the premises of a cement plant in eastern Slovakia. The aim is to present a complete workflow for data processing from field measurement to a 3D model and quantitative analysis of the geometric parameters of the objects, including the determination of height characteristics, diameter, verticality, and deviations from the ideal cylindrical and vertically oriented cylindrical model.

Material and methods

Study area. The measurements for our research were carried out in an industrial plant, specifically a cement plant. Homogenization silos play an important role in the cement production process. From a geometric perspective, they are tall vertical structures with a predominantly cylindrical shape. The silos are approximately 90 m high (Fig. 1).

Fig. 1. View of the cement plant and the object of research
Source: DANUCEM

Surveying equipment. A terrestrial laser scanner, Leica RTC360, was used for the acquisition of spatial data. The device operates on the time-of-flight principle and, according to the technical specifications (Table 1), can record up to 2,000,000 points per second within a measurement range of 0.5 to 130 m. The scanner provides a horizontal field of view of 360° and a vertical field of view of 300°, which enables efficient capture of a large portion of the surrounding space from a single scan position. The device is equipped with an HDR camera system and VIS technology, which supports subsequent registration between scan positions.

For determining the spatial position of reference points, a Leica GS12 GNSS receiver with a Leica CS15 field controller was used. The measurements were carried out in RTK mode with a 30-second observation on each point and were used to survey targets serving as Ground Control Points (GCPs) and Check Points (CPs) for georeferencing the final point cloud. The accuracy of the GNSS measurements is up to 20 mm in both position and height.

Table 1. Specification of TLS Leica RTC 360

General	Terrestrial laser scanner, HDR, VIS
Distance measurement	Time-of-Flight
Speed	2,000,000 points/s
Range	0.5 – 130 m
Field of view	360° horizontal, 300° vertical
Angular accuracy Range accuracy	18´´ 1.0 mm + 10 ppm
3D point accuracy	1.9 mm at 10 m; 2.9 mm at 20 m; 5.3 mm at 40 m
Resolution	3/6/12 mm at 10m
Noise	0.4 mm at 10m, 0.5mm at 20m

Source: own elaboration based on Leica RTC360, 2026

Software. Data processing was carried out in several software environments, each serving a specific role. Leica Cyclone REGISTER 360 was used for scan import, registration, and georeferencing. Trimble RealWorks was used for point cloud preprocessing, cropping, density reduction, segmentation, data cleaning, cross-section generation and circle fitting. CloudCompare was used for and the creation of a polygonal model. Leica Cyclone 3D was used for the analysis of the geometric parameters of the silos' surfaces in comparison with an ideal cylindrical model.

This software combination made it possible to separate the individual stages of the workflow and to exploit the advantages of tools designed for specific types of operations. At the same time, it ensured control over the results at different stages of processing.

Data collection. The scan station layout was designed to ensure sufficient overlap between individual scans while minimizing occlusions caused by technological elements surrounding the silos. Scanning was performed from ground level as well as from stations located on steel structures and buildings at different height levels, covering the full height of the object. In total, 57 scans were acquired. The distribution of scanning stations is shown on Fig. 2.

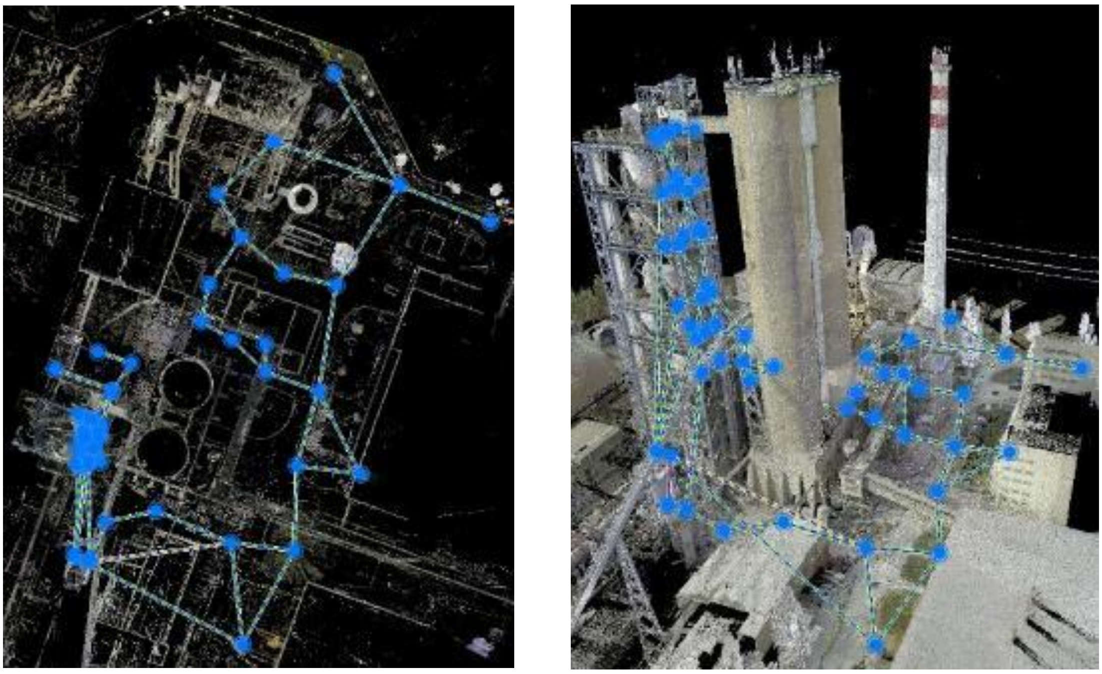

(a) (b)

Fig. 2. Scanning positions – top view (a), side view (b)
Source: own elaboration

Reference targets (GCPs and CPs) were placed at 11 stations for georeferencing and point cloud quality control (Fig. 3).

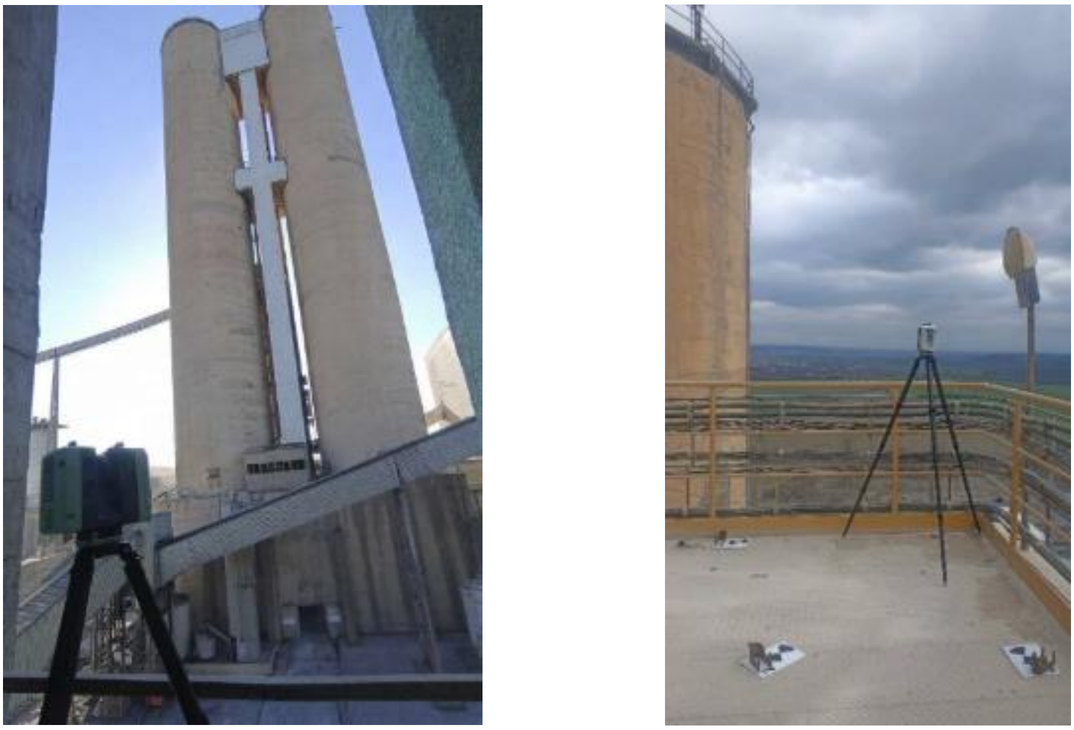

Fig. 3. Scan positions of TLS during the scanning of the homogenization silos
Source: own elaboration

Scan registration and georeferencing. After importing the data into Leica Cyclone REGISTER 360, the single scans were gradually registered into a common project. The registration was based on the mutual overlap of the scans, and its refinement was carried out using the software's optimization tools (Fig. 4).

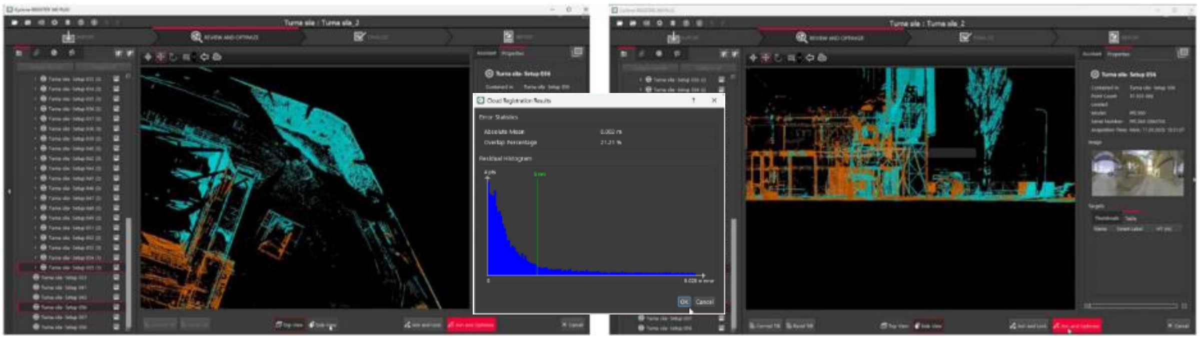

(a) (b)

Fig. 4. Scan registration – top view (a), side view (b)
Source: own elaboration

For georeferencing, GCPs represented by the centers of black-and-white targets determined by RTK GNSS were used. The coordinate system used was System of the Unified Trigonometrical Cadastral Network (S-JTSK) in the JTSK realization, and the height system was Baltic after adjustment (Bpv). Seven points were included in the final transformation. The resulting registration metrics reached 5 mm for both bundle error and cloud-to-cloud error. The overall scan overlap reached 55%. These values indicate that the resulting point cloud provided a sufficiently reliable basis for the subsequent analysis (Fig. 5).

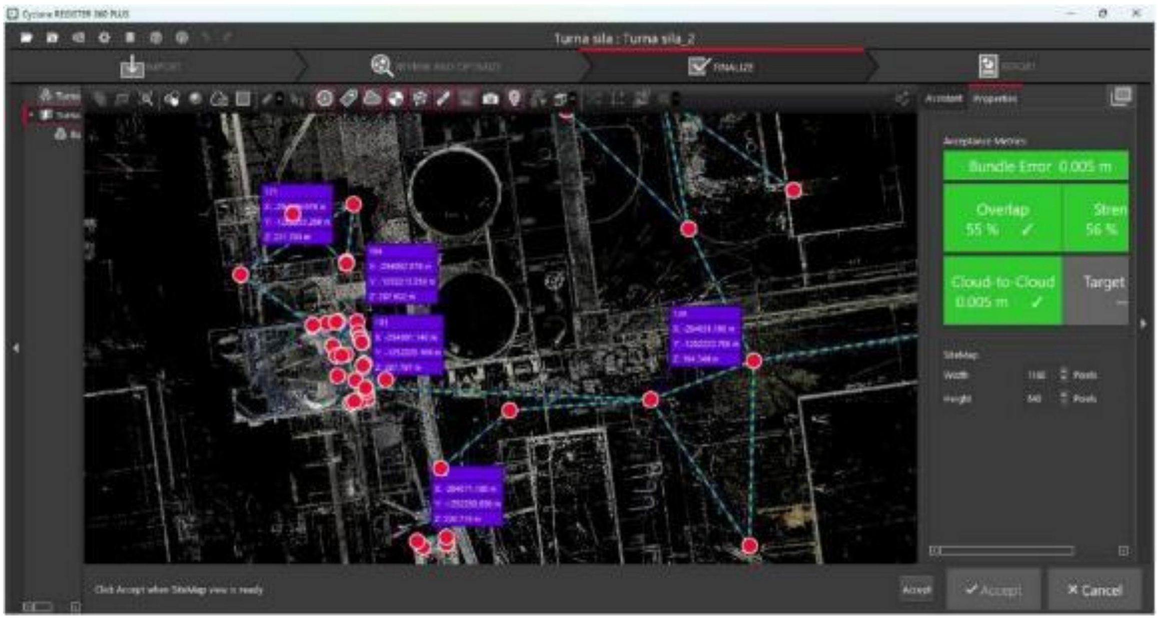

Fig. 5. Results of point cloud registration and accuracy parameters
Source: own elaboration

Preprocessing of the data and creation of the 3D model. After registration, the resulting point cloud containing 2.1 billion points was exported as E57 and LAS formats and preprocessed in Trimble RealWorks. At this stage, irrelevant parts of the scene and technological elements outside the scope of the analysis were removed, and the point density was reduced and homogenized. Spatial sampling was set to 10 mm and 50 mm, and the point cloud with a final resolution of 50 mm containing 2,409,754 points was used for further processing (Fig. 6). Primary segmentation was performed using Trimble Realworks software to separate the analyzed silos from the surrounding scene. Subsequent cleaning was carried out using the SOR filter using CloudCompare, which eliminated outlier points and local noise. After computing normals with a search radius of 0.2 m, a polygonal model was generated using the Poisson Surface Reconstruction algorithm.

Fig. 6. Georeferenced TLS point cloud of the investigated homogenization silos
Source: own elaboration

Geometric analysis workflow. Geometric analysis was carried out separately for each silo based on the cleaned point cloud. Disturbing elements and the basement of the objects were removed from the input data so that the results were not affected by points unrelated to the geometry of the silo shells (Fig. 7).

The object height was determined from the extreme values of the Z coordinate. To assess the diameter and the course of the axis, horizontal cross-sections with a thickness of 0.1 m and interval of 5 m were created. A total of 18 sections were generated for each object, and in each section (Fig. 8), circle fitting was performed using the least squares method. The horizontal displacement of the axis and its deviation from the vertical were then determined from the coordinates of the circle centers.

Fig. 7. Filtered and cleaned point cloud used for geometric analysis
Source: own elaboration

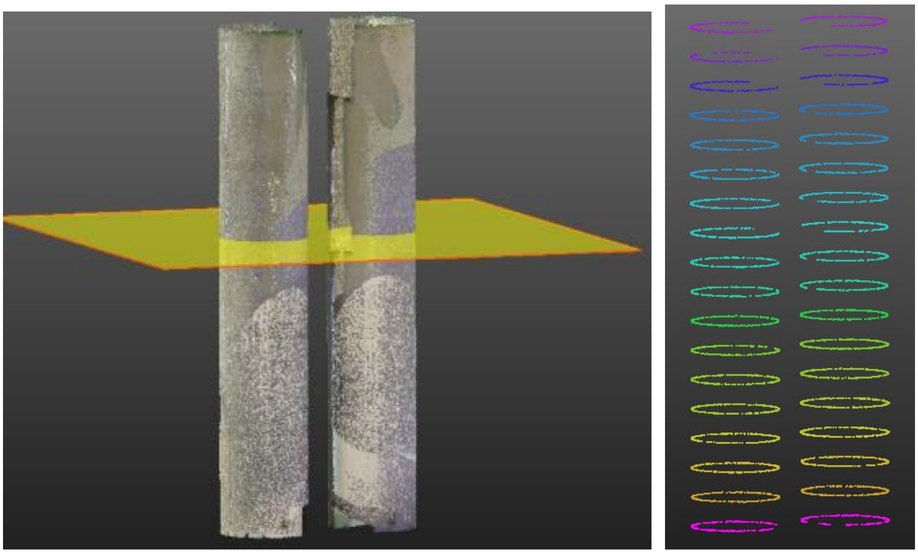

(a) (b)

Fig. 8.Generation of horizontal cross-sections for geometric analysis – cutting plane (a), resulting cross-sections (b)
Source: own elaboration

Results

Heights of the objects based on TLS point clouds. The height parameters of the objects were derived from the georeferenced point cloud. During interpretation, it was important to distinguish the maximum height of the silo body itself from the maximum height of the object including technological elements located at the top, especially antennas (Fig. 9 and Table 2).

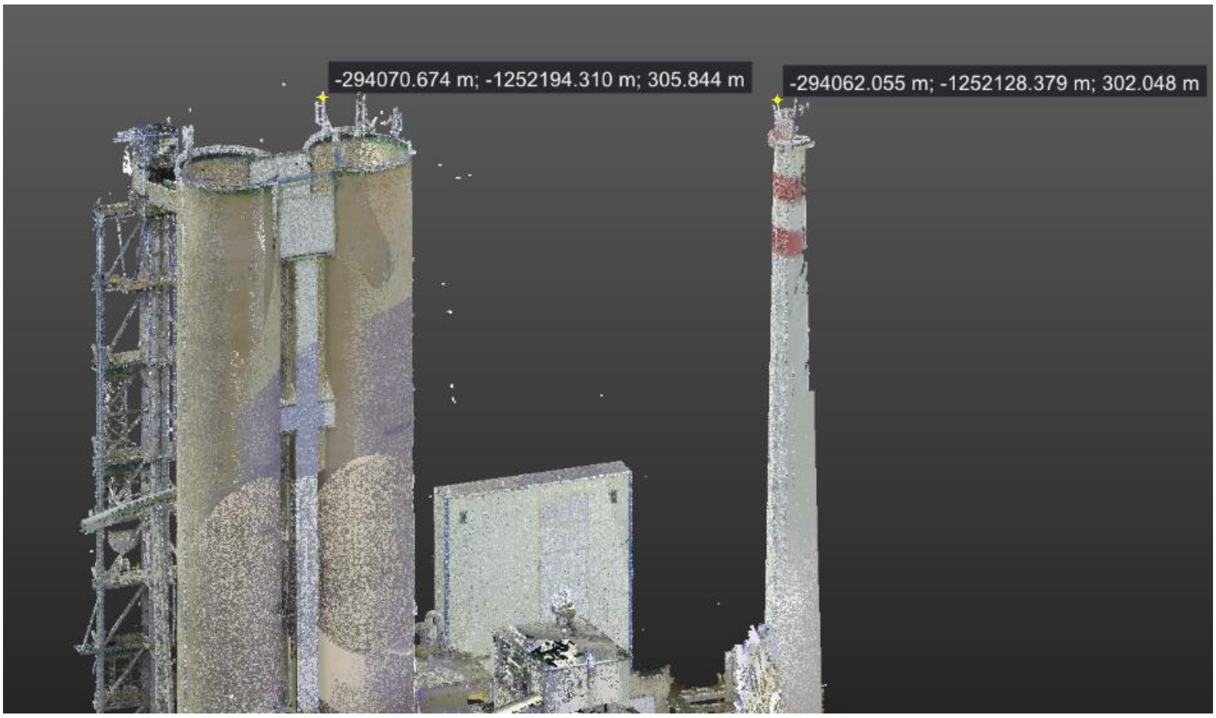

Fig. 9. Height determination from TLS point cloud
Source: own elaboration

Table 2. Heights derived from TLS point cloud

Object	Z_{min} [m]	Z_{max} [m]	Z_{silo} [m]	H_{silo} [m]	$H_{overall}$ [m]
southern silo	210.500	305.497	298.445	87.945	94.997
northern silo	210.500	306.930	298.447	87.947	96.430

Source: own elaboration

Centers of the cross-sections and silo diameters. The range of cross-sections used for the subsequent analysis was defined between elevation levels of 212 m and 297 m, corresponding to an interval of 85 m. This interval also served as a common basis for assessing the verticality of both silos.

Circle fitting of the cross-sections showed that the diameters of both objects varied only minimally over their full height. This indicates a high regularity of their basic geometry and a good agreement with the assumed cylindrical model. The following results are presented only for the southern silo (Table 3).

Evaluation of the verticality of the silos. The verticality of the objects was assessed from the coordinates of the circle centers in the lowest and highest analyzed sections. This approach made it possible to quantify the spatial displacement of the axis in the horizontal plane and convert it into the angle of deviation from the vertical.

Table 3. Parameters of the fitted circles for the cross-sections of the southern silo

Cross-section number	Z[m]	X [m]	Y [m]	R [m]	D [m]
1	212.000	294,061.883	1,252,210.872	7.411	14.822
2	217.000	294,061.878	1,252,210.880	7.416	14.832
3	222.000	294,061.888	1,252,210.891	7.414	14.828
4	227.000	294,061.904	1,252,210.891	7.418	14.836
5	232.000	294,061.919	1,252,210.885	7.411	14.821
6	237.000	294,061.930	1,252,210.893	7.414	14.828
7	242.000	294,061.938	1,252,210.911	7.417	14.835
8	247.000	294,061.944	1,252,210.925	7.417	14.835
9	252.000	294,061.962	1,252,210.938	7.419	14.838
10	257.000	294,061.985	1,252,210.943	7.412	14.824
11	262.000	294,061.988	1,252,210.961	7.418	14.837
12	267.000	294,062.006	1,252,210.988	7.418	14.836
13	272.000	294,062.012	1,252,211.002	7.420	14.840
14	277.000	294,062.024	1,252,211.004	7.416	14.832
15	282.000	294,062.038	1,252,210.987	7.413	14.826
16	287.000	294,062.024	1,252,210.970	7.421	14.843
17	292.000	294,062.051	1,252,210.995	7.418	14.836
18	297.000	294,062.075	1,252,211.051	7.414	14.828

Source: own elaboration

For the southern silo, a horizontal axis displacement of 0.262 m was determined over a height difference of 85 m. This corresponded to a deviation angle from the vertical of 0.177°, i.e., approximately 0° 10′ 36″ (Table 4). The graphical representation of the results is shown in Fig. 10.

Table 4. Horizontal deviations of the circle centers from the ideal vertical axis for the southern silo

Cross-section number	Z[m]	X [m]	Y [m]	ΔX [m]	ΔY [m]	d [m]
1	212.000	294,061.883	1,252,210.872	0.000	0.000	0.000
2	217.000	294,061.878	1,252,210.880	-0.005	0.008	0.009
3	222.000	294,061.888	1,252,210.891	0.005	0.019	0.020
4	227.000	294,061.904	1,252,210.891	0.021	0.019	0.028
5	232.000	294,061.919	1,252,210.885	0.036	0.013	0.039
6	237.000	294,061.930	1,252,210.893	0.047	0.021	0.052
7	242.000	294,061.938	1,252,210.911	0.056	0.039	0.068
8	247.000	294,061.944	1,252,210.925	0.061	0.053	0.081
9	252.000	294,061.962	1,252,210.938	0.079	0.066	0.103
10	257.000	294,061.985	1,252,210.943	0.102	0.071	0.124
11	262.000	294,061.988	1,252,210.961	0.105	0.089	0.138
12	267.000	294,062.006	1,252,210.988	0.123	0.116	0.169
13	272.000	294,062.012	1,252,211.002	0.129	0.130	0.183
14	277.000	294,062.024	1,252,211.004	0.141	0.132	0.193
15	282.000	294,062.038	1,252,210.987	0.155	0.115	0.193
16	287.000	294,062.024	1,252,210.970	0.141	0.098	0.172
17	292.000	294,062.051	1,252,210.995	0.168	0.123	0.208
18	297.000	294,062.075	1,252,211.051	0.192	0.179	0.262

Source: own elaboration

Shell deviations vs. cylindrical model. The comparison of the surface of the analyzed objects with the best-fit cylindrical and vertical cylindrical model was carried out in Trimble RealWorks (Fig. 11). For best-fit cylinder RMSE fitting value reaches 37 mm. Other parameters are in Fig. 11a.

Vertical cylinder was constructed using the lowest cross-section at a height of 212 m, with the diameter taken from the best fit, i.e. 14.833 m. Other parameters are in Fig. 11b.

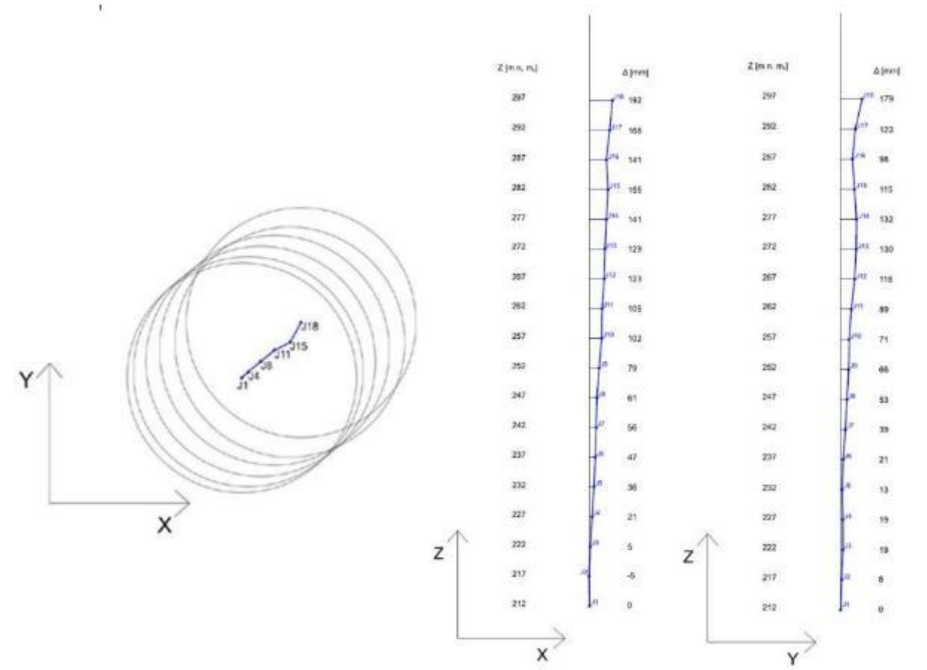

Fig. 10. Graphical interpretation of verticality – southern silo
Source: own elaboration

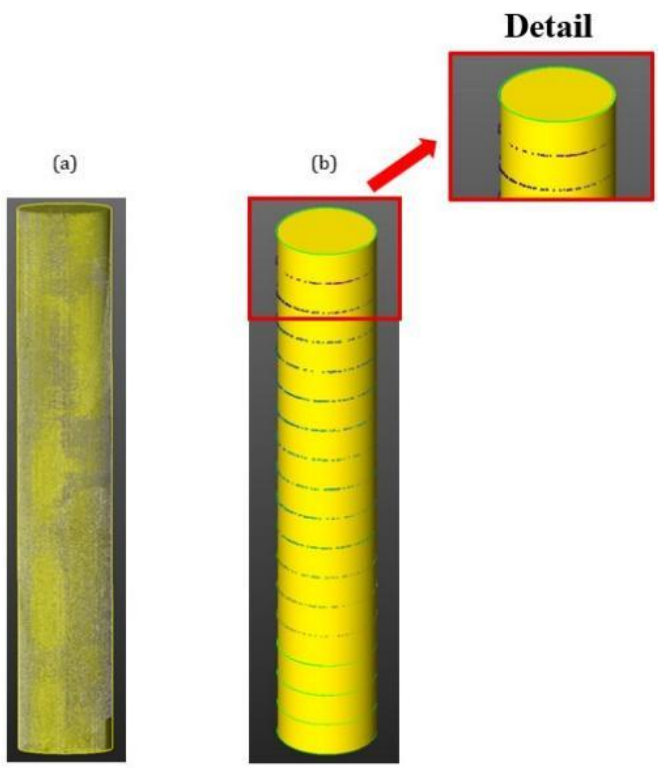

	best fit cylinder	vertical cylinder
type	cloud-based	3D geometry
fit RMSE	37 mm	-
Z axis	0.002; 0.002; 1.000	0.000; 0.000; 1.000
radius	7.416m	7.416m

Fig. 11. Cylinder fitting (southern silo) – best fit (a), vertical cylinder (b)
Source: own elaboration

Results are shown as differential models with numerical values in Fig. 12.

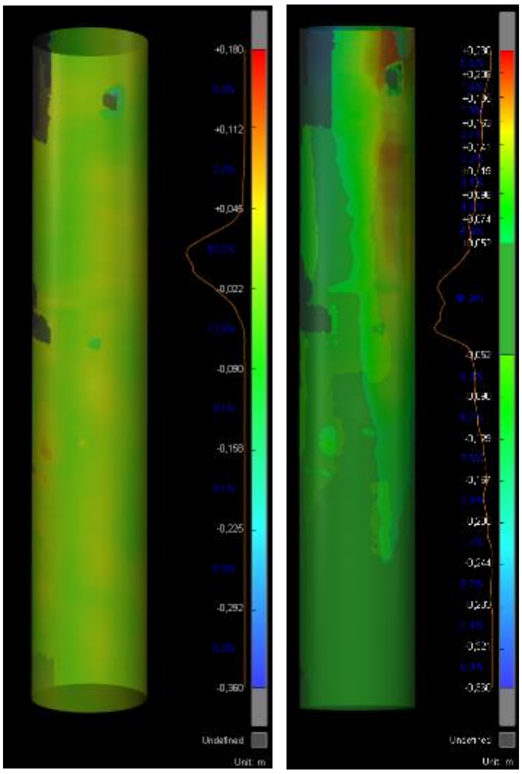

(a) (b)

Fig. 12. Differential model (southern silo) – shell versus best-fit cylinder (a),
shell versus vertical cylinder (b)
Source: own elaboration

The results showed that the detected deviations were predominantly local. They were mainly related to structural details, local surface irregularities, and partly also to the slight spatial displacement of the object axes. Fig. 12a shows a differential model against a reference best-fit cylinder. The values of interest span the interval from –30 mm to +40 mm, containing 84% of filtered points. Based on these values, the computed ovality is 0.94%. Fig. 12b shows the deviations (consistent with Table 4 and Figure 10) using a differential model. For the assessment of the silo's verticality, the extreme values of the colour scale need to be considered. The maximum vertical deviation (tilt) value of the silo reaches 262 mm.

Discussion and future work

The presented workflow confirms that TLS is a suitable tool for documenting large industrial objects, where it is necessary to analyze not only basic dimensions, but also form characteristics and surface deviations. A key factor for the success of such a workflow is an appropriate scan-station layout, sufficient overlap between scans, and a combination of tools that enables registration, data cleaning, and subsequent analytical interpretation.

From a methodological point of view, it is important to distinguish between the visualization model and the analytical data. The polygonal model created by Poisson reconstruction is well suited for visual presentation of the object; however, for quantitative analysis of geometric parameters, cleaned point clouds have greater informative value because they preserve the original measured positions without additional interpolation.

The obtained results are consistent with previous studies demonstrating the suitability of TLS for geometric analysis and documentation of large technical and industrial structures. Kovanič et al. (2020) demonstrated the applicability of TLS point-cloud segmentation for the analytical determination of geometric parameters of a rotary kiln, while Kovanič et al. (2023) confirmed the potential of combining TLS and UAS photogrammetry for determining geometric parameters of large-scale industrial facilities. Similarly, Erdélyi et al. (2020, 2022) showed that point-cloud-based methods can provide reliable geometric information for the assessment and verification of engineering structures. Compared with these studies, the presented approach focuses specifically on cylindrical industrial structures and extends the analysis from basic geometric parameters to verticality and deviations from an ideal cylindrical model. The results therefore confirm that TLS provides a suitable basis for detailed geometric assessment of large industrial objects.

The results also show that even for objects with a relatively simple basic geometry, it is necessary to carefully remove disturbing elements and to select cross-section intervals appropriately. Poorly chosen sections or the retention of technological details in the input data could negatively affect the estimates of diameter and verticality.

One limitation of the processing is the manual character of some steps, especially the extraction of circle parameters and their subsequent evaluation. In future research, it would be appropriate to extend the workflow with automated scripts for batch export of section parameters, statistical evaluation of deviations, and comparison of the object in order to monitor possible changes in geometry over time.

Conclusions

The article presents a workflow for data acquisition and processing using terrestrial laser scanning in the creation of a 3D model and the analysis of geometric parameters of homogenization silos located in a cement plant. Based on 57 scans, GNSS georeferencing, and multi-stage processing in Leica Cyclone, Trimble RealWorks, and CloudCompare, it was possible to create a unified point cloud, a polygonal model, and analytical inputs for assessing height, diameter, verticality, and shell shape deviations.

The results showed that the analyzed objects exhibit a high degree of geometric regularity, a very stable diameter over height, and only a slight deviation from the vertical axis. The detected deviations were predominantly local in nature and were mainly related to structural details and slight spatial displacement of the axes. The presented workflow confirms the suitability of TLS for the documentation and analytical evaluation of similar industrial structures.

Acknowledgements

This research was supported by the Slovak Research and Development Agency under contract KEGA grant no. 018TUKE-4/2026, 011TUKE-4/2024, grant no. APVV-18-0351 and Interreg grant #mountgreenfra – HUSK/2302/1.2/060.

Declaration of competing interests

The authors declare that they have no known competing financial interests or personal relationships that could have appeared to influence the work reported in this paper.

Data availability

The datasets used and analyzed during the current study are available from the corresponding author upon reasonable request.

Use of generative AI and AI-assisted technologies

Generative AI tools were used only for language editing and grammar improvement. The authors reviewed and approved all final content.

References

Bakuła K., Pilarska M., Salach A., Kurczyński Z. (2020). Detection of Levee Damage Based on UAS Data – Optical Imagery and LiDAR Point Clouds. ISPRS International. Journal of Geo-Information*, 9,* 248. https://doi.org/10.3390/ijgi9040248.

Bariczová G., Erdélyi J., Honti R., Tomek L. (2021). Wall Structure Geometry Verification Using TLS Data and BIM Model. Applied Sciences, 11, 11804. https://doi.org/10.3390/app112411804.

DANUCEM https://www.betonserver.sk/danucem-cementaren-turna#gallery-2 [access: 15.02.2026].

Erdélyi J., Honti R., Funtík T., Mayer P., Madiev A. (2022). Verification of Building Structures Using Point Clouds and Building Information Models. Buildings, 12, 2218. https://doi.org/10.3390/buildings12122218.

Erdélyi J., Kopáčik A., Kyrinovič P. (2020). Spatial Data Analysis for Deformation Monitoring of Bridge Structures. Applied Sciences, 10, 8731. https://doi.org/10.3390/app10238731.

Gajski D., Dzięgielewska-Gajski K. (2023). Nadir & Oblique Aerial Imagery – New Possibilities in 3D Mapping. GIS Odyssey Journal, 3(1), 137–147. https://doi.org/10.57599/gisoj.2023.3.1.137.

Gajski D., Peloza M., Dzięgielewska-Gajski K. (2026). Artificial Intelligence in Photogrammetric Measuring and Modelling of Landslide Events. GIS Odyssey Journal, 6(1), 263–279. https://doi.org/10.57599/gisoj.2026.6.1.263.

Geotech s.r.o. 2026. Leica GS07. https://www.geotech.sk/Produkty/GPS-GNSS/Leica-GS07.html [access: 27.06.2026].

Geotech s.r.o. 2026. Leica RTC360. https://www.geotech.sk/Produkty/Laserove-skenery-HDS/Leica-RTC360.html [access: 27.06.2026].

Kovanič Ľ., Blišťan P., Topitzer B., Peťovský P., Boczek R. (2023). TLS And Low-Cost UAV Photogrammetry as an Effective Combination of Spatial Data Collection Methods for Creating Detailed 3D Surface Models (DEM). GIS Odyssey Journal, 3(1), 163–178. https://doi.org/10.57599/gisoj.2023.3.1.163.

Kovanič Ľ., Štroner M., Blišťan P., Urban R., Boczek R. (2023). Combined Ground-Based and UAS SfM-MVS Approach for Determination of Geometric Parameters of the Large-Scale Industrial Facility – Case Study. Measurement, 216, 112994. https://doi.org/10.1016/j.measurement.2023.112994.

Kovanič Ľ., Blišťan P., Urban R., Štroner M., Pukanská K., Bartoš K., Palková J. (2020). Analytical Determination of Geometric Parameters of the Rotary Kiln by Novel Approach of TLS Point Cloud Segmentation. Applied Sciences, 10, 7652. https://doi.org/10.3390/app10217652.

Kregar K., Marjetič A., Savšek S. (2022). TLS-Detectable Plane Changes for Deformation Monitoring. Sensors, 22, 4493. https://doi.org/10.3390/s22124493.

Ma L., Li Y., Li J., Wang C., Wang R., Chapman M.A. (2018). Mobile Laser Scanned Point-Clouds for Road Object Detection and Extraction: A Review. Remote Sensing, 10, 1531. https://doi.org/10.3390/rs10101531.

Mackiewicz E. (2021). Management of the Renovation of Monuments to Optimise the Buildings Utility Values and Energy Efficiency (Case Study Rzuchów, Poland). GIS Odyssey Journal, 1(2), 31–45. https://doi.org/10.57599/gisoj.2021.1.2.31.

Matoušková E., Pavelka K., Smolík T., Pavelka K., Jr. (2021). Earthen Jewish Architecture of Southern Morocco: Documentation of Unfired Brick Synagogues and Mellahs in the Drâa-Tafilalet Region. Applied Sciences, 11, 1712. https://doi.org/10.3390/app11041712.

Pavelka K., Matoušková E., Pavelka K., Jr. (2023). Remarks on Geomatics Measurement Methods Focused on Forestry Inventory. Sensors, 23, 7376. https://doi.org/10.3390/s23177376.

Štroner M., Křemen T., Urban R. (2022). Progressive Dilution of Point Clouds Considering the Local Relief for Creation and Storage of Digital Twins of Cultural Heritage. Applied Sciences, 12, 11540. https://doi.org/10.3390/app122211540.

Štroner M., Urban R., Křemen T., Braun J., Michal O.; Jiřikovský T. (2025). Scanning the underground: Comparison of the accuracies of SLAM and static laser scanners in a mine tunnel, Measurement, vol. 242, part A, 2025, 115875. https://doi.org/10.1016/j.measurement.2024.115875.

Urban R., Štroner M., Braun J., Suk T., Kovanič Ľ., Blišťan P. (2024). Determination of Accuracy and Usability of a SLAM Scanner GeoSLAM Zeb Horizon: A Bridge Structure Case Study. Applied Sciences, 14, 5258. https://doi.org/10.3390/app14125258.